

Anomalous transport in Charney-Hasegawa-Mima flows

Xavier Leoncini¹, Olivier Agullo¹, Sadruddin Benkadda¹, and George M. Zaslavsky^{2,3}

¹ PIIM, Université de Provence, CNRS, Centre Universitaire de Saint Jérôme, F-13397 Marseilles, France, e-mail: Xavier.Leoncini@up.univ-mrs.fr

² Courant Institute of Mathematical Sciences, New York University, 251 Mercer St., New York, NY 10012, USA

³ Department of Physics, New York University, 2-4 Washington Place, New York, NY 10003, USA

Received: date / Revised version: date

Abstract. Transport properties of particles evolving in a system governed by the Charney-Hasegawa-Mima equation are investigated. Transport is found to be anomalous with a non linear evolution of the second moments with time. The origin of this anomaly is traced back to the presence of chaotic jets within the flow. All characteristic transport exponents have a similar value around $\tau = 1.75$, which is also the one found for simple point vortex flows in the literature, indicating some kind of universality. Moreover the law $\tau = \tau_0 + 1$ relating the transport exponent to the trapping time exponent within jets is confirmed and an accumulation towards zero of the spectrum of finite time Lyapunov exponent is observed.

PACS. 05.45.Ac

1 Introduction

Understanding transport in turbulent magnetized plasma is a task of fundamental importance. In these plasma, transport problems are often related to confinement, which is one of the last standing issues confronting the realization of magnetically confined controlled fusion devices. As the literature evolves, there has been more and more evidence showing that the transport properties can be anomalous, in the sense that transport may not be correctly described by Gaussian kinetics, but by what one now calls “strange kinetics” [1]. In these regards, transport phenomena in turbulent magnetized plasma is part of the ever growing number of physical systems displaying anomalous properties [2,3,4,5]. As of today the full understanding of these phenomena are far from being complete and in many regards a full blown theory able to capture and describe correctly these “strange kinetics” has not yet surfaced. There seems although a common agreement to link these phenomena to Levy-type processes and their generalizations, moreover the use of fractional derivatives in Fokker-Plank-Kolmogorov type equations captures qualitatively some of the transport properties and is thus a good step towards a proper description of anomalous transport [6].

The link between the Hamiltonian dynamics and the kinetics at origin of anomalous transport properties are relatively well understood when dealing with low dimensional systems such as a time periodic flow which belong to the class of $1 - 1 = 2$ degree of freedom Hamiltonians. The dynamics in these systems is not ergodic: a well-defined stochastic sea, with chaotic dynamics, filled with

various islands of quasi-periodic dynamics compose the phase space. The anomalous properties and their multi-fractal nature are then linked to the existence of islands within the stochastic sea and the phenomenon of stickiness observed around them [7,8]. However when dealing with more complex systems the loss of time-periodicity complicates the picture. For instance in geophysical flows or two-dimensional plasma turbulence, the islands which were static and well localized in phase space, are replaced by “coherent structures”, which have a life of their own. Hence, tackling the origin of anomalous transports from the chaotic dynamics of individual tracers becomes more subtle. Recently, the existence of a hidden order for the tracers which exhibits their possibility to travel in each other vicinity for relatively large times was exhibited [9]. This order is related to the presence within the system of chaotic jets [10,11]. These chaotic jets can be understood as moving clusters of particles within a specific domain for which the motion appears as almost regular from a coarse grained perspective. Typically, the chaotic motion of the tracers is confined within the characteristic scale of a given jet, within which nearby tracers are trapped. From another point of view, looking for chaotic jets can be understood as a particular case of measurements of space-time complexity [12].

The purpose of this paper is to study transport properties and to look for chaotic jets in a model of two-dimensional turbulence which applies either in the plasma context where it is known as the Hasegawa-Mima equation [13] or in the geophysical one where one talk about the Charney equation (see for instance [14]). In this setting Annibaldi et al have already shown strong evidence

of anomalous transport of passive particles [3,15], hence the search for chaotic jet is expected to give some clues on the origin of anomalous transport in these systems, and for instance to identify the structures responsible for such transport. Indeed in [9], it was clearly shown that trapping within chaotic jets was resulting in anomalous transport, moreover it appeared that jets were localized around the coherent structures of systems, namely the vortex cores and that the structure of the jets itself was a hierarchy of jets within jets, reminiscent of the multi-fractal nature of transport observed in 1–2 degree of freedom Hamiltonians systems [8]. Hence, the goal of this paper may be seen as two-fold, we want to understand the origin of anomalous transport in a model of two-dimensional plasma turbulence, and since we are using chaotic jets to track this origin, we are at the same time testing the existence of these jets in a more complex setting than the system of point vortices used in [9]. If the existence is confirmed we may expect that the different anomalous transport behavior portrayed in the nonexhaustive following references [16,2,17,18,19,20] may all find their origin in the presence of long lived chaotic jets in the considered systems.

The paper is organized as follows, in Sec. 2 the basic definitions are introduced. A brief introduction of the Charney-Hasegawa-Mima equation is given, then the dynamics of test particles is given and the Lagrangian approach of transport in this setting discussed. In Sec. 3 the dynamical evolution of the field and of passive test particles as well as transport properties are computed numerically. First the numerical setting is discussed, then three different regimes corresponding to different choices of the parameters for the field evolution are considered. In Sec. 4 We track the origin of anomalous transport in the three cases considered, first we recall the definition of a chaotic jet and present the numerical method used to detect these jets. We then present the statistical results related to trapping time within jets and analyze the origin of anomalous transport by localizing the jets and looking at their structure. Finally we conclude in Sec. 5.

2 Basic definitions

2.1 The Charney-Hasegawa-Mima equation

The Charney-Hasegawa-Mima equation can be written in the following form,

$$\partial_t + [;] = 0 \quad (1)$$

$$= + g x ; \quad (2)$$

where $[;]$ corresponds to the Poisson operator, ∂_t is a generalized vorticity given by Eq.(2), ∂_t is a potential and g and ∂_t are parameters.

Typically Eqs. (1) and (2) can either describe the evolution of an anisotropic plasma, and are then referred to as the Hasegawa-Mima equation or the evolution of geostrophic flows in which context they are known as the Charney equation. This formal identity has an advantage

as the results obtained in this paper for transport properties being agnostic, they should apply in either context.

It is however important to be able to put the results back in a physical context, with this in mind we provide in the next section a short derivation of Eqs (1) and (2) in both the anisotropic plasma configuration and the geostrophic approximation.

2.2 Wave-vortex paradigm equation for two-dimensional flows.

2.2.1 The Hasegawa-Mima equation

Let us start by considering an anisotropic plasma, *i.e* a plasma with a uniform magnetic field along a direction, $B = B z$. We shall also assume that electron response to the turbulent fluctuations of the electric potential ϕ is adiabatic, $n_e(x; y; t) = n_0(x; y) e^{-(x^2 + y^2)/T_e}$, where n_e is the electron density, n_0 is the equilibrium plasma density, and T_e the electrons temperature. Being in an anisotropic plasma, we shall consider as well the cyclotron frequency $\omega_c = eB/m_e$ and the hybrid sound speed $c_s = \sqrt{T_e/m_i}$.

We now consider the motion of cold ions (the ion temperature is assumed zero, $T_i = 0$) on characteristic time and length scale much larger respectively than $1/\omega_c$ and the Debye length λ_D . In this situation the plasma is quasi-neutral $n_i = n_e$, and a linear combination of ion continuity equation and momentum equations gives (see [21] for details)

$$r \cdot \nabla v_\perp = \frac{D}{D t} \frac{e}{T_e} + v_\perp \cdot \nabla \ln n_0 = \frac{1}{1 + \omega_c^2 D^2} (1 + \omega_c^2) ; \quad (3)$$

where v_\perp is the speed in the plane perpendicular to the magnetic field and $\omega = \nabla \times v_\perp$ is the vorticity of the 2D flow. The slow motion of the ions necessarily implies that $v_\perp = v_B = B_0^{-1} z$ and, using the notation $\omega = \omega_e = T_e^{-1}$, subtraction of the right terms in (3) readily gives

$$\frac{D}{D t} (4 \omega' - \omega' = \frac{\omega^2}{\lambda_L^2}) - v_B \cdot \nabla \ln n_0 = 0 ; \quad (4)$$

where $\lambda_L = c_s/\omega_c$ is the hybrid Larmor radius.

When the plasma is homogeneous ($n_0 = Cte$), the turbulent dynamics of (4) is characterized by the absence of waves and the formations of large vortices, moreover, in the $\lambda_L \ll 1$ limit, Eq. (4) becomes formally equivalent to the 2D momentum Euler equation (ω' being the stream function in the Euler case).

In plasma devices, the equilibrium profile of density is larger in the core than at the boundaries. We can therefore write $n_0(x; y) = n_0 e^{-x^2/L_n^2}$, where L_n is a characteristic density gradient length to finally obtain the well-known Hasegawa-Mima equation:

$$\frac{D}{D t} (4 \omega' - \omega' = \frac{\omega^2}{\lambda_L^2}) - g \frac{\partial \omega'}{\partial y} = 0 ; \quad (5)$$

where $g = \omega_c^2/L_n^2$.

The inhomogeneous character of the equilibrium density profile in Eq.(5) implies the existence of waves in the flow. In particular, those drift waves deform and interact with the self-organized vortex-like or multipole-like structures and play a key role in their interactions, for instance the collision of two dipoles can lead to two monopoles plus one dipole plus some radiation [22].

2.2.2 The Charney Equation

Let us now precise the physical nature of the intrinsic length in atmosphere motions. In the context of the shallow water approximation where the density is uniform (density stratification is not taken into account), modeling of the atmospheric turbulence leads to a dynamic equation similar to (3) or (5). Indeed, the atmosphere is characterized by small Ekman and Rossby numbers[14], so that the motion of an thin incompressible fluid rotating layer (thin with respect to the characteristic scale L_2 of the horizontal motion) is such that, first, friction forces are very weak compare with the inertial Coriolis' one, second, pressure forces are balanced by gravity in the vertical direction z (hydrostatic approximation). As a consequence the horizontal pressure gradient is independent of the vertical component z , proportional also to the layer width $h(x; y; t)$ (because of the free boundary condition $p(x; y; h) = p_0 = \text{Cte}$) and it is therefore reasonable to assume that the horizontal velocity field $v_?$ is also z -independent: $v = v_? (x; y; t) + w (x; y; z; t)z$.

If we assume that the rigid earth surface is locally flat, i.e $w(z = 0) = 0$, integration of the incompressibility condition leads to $w = -zr v_?$ and, in particular, $dh=dt = -hr v_?$. Moreover, the forces acting on the fluid being the Coriolis and pressure forces, $f v_? - z$ and $-r p$, it is straightforward to deduce from the momentum equation the exact identity $d(! + f)dt = (! + f)r v_?$. It follows that

$$r v_? = \frac{D}{Dt} \frac{h}{H_0} = \frac{1}{! + f} \frac{D}{Dt} (! + f); \quad (6)$$

where we put $h = h + H_0$, H_0 being the mean width of the layer and h the fluctuations around the mean ($h = H_0$ by hypothesis). The Coriolis term fz is the local component of the planetary vorticity $!_planet$ in the vertical direction, the northward local component $f_n y$ being negligible. Indeed, the Coriolis force in the horizontal direction is $(2 !_planet v_?) = v_? f z + w z f y$ $v_? f z$ because, in the shallow water approximation, $w = v_? = 0 (H_0 = L_2) = 1$ and far from equator latitudes, $f_n = f$.

It is clear from equations (3) and (6) that in the special limits where the plasma is homogeneous ($n_0 = \text{Cte}$) and the Coriolis parameter $f = f_0$ is taken constant, both physical systems are formally equivalent. We just have to identify $e = T_e$ with $h = H_0$ and choose as length and time units $(L_2; 1 = !_c)$ or $(L_2; 1 = f_0)$, where $L_2 = \frac{1}{gH_0} = f_0$ is the so-called Rossby length. But the similarity holds even for a case of a layer with a slow dynamics ($! + f$) by taking

into account the slow variation of the Coriolis parameter in the northward y -direction: $f = f_0 + y$ with $f = f_0$ 1 (- plane approximation). In fact, because the Rossby number is small, we can also make the approximation $v_? = v_0 = g f^{-1} z - r h$. And by subtracting the right terms of (6), we obtain the so-called Charney equation

$$\frac{D}{Dt} (4 h - h^2) - \frac{\partial h}{\partial y} = 0; \quad (7)$$

It is clear that (5) and (7) are formally equivalent. However, in the atmospheric case, waves are not generated by a density inhomogeneity but by the earth rotation. As mentioned earlier, both equations (5) and (7) can be written in the compact form given by (1) where Eq.(2) actually writes $= ' \frac{!}{L_2} ' x = L_2$ (the transformations $' \frac{!}{L_2} h$, $g f^{-1} z$, and L_2 lead to the Charney equation).

2.3 Advection equation

For an incompressible fluid, the evolution of a passive particle is given by the advection equation

$$z = v(z; t) \quad (8)$$

where $z(t)$ represent the position of the tracer at time t in the complex plane, and $v(z; t)$ is the velocity field. An important feature of this evolution of passive particles is that the evolution equation given Eq.(8) can be rewritten as:

$$z = \frac{\partial}{\partial z}; \quad z = i \frac{\partial}{\partial z}; \quad (9)$$

where the potential ϕ acts as a time dependant Hamiltonian. This Hamiltonian structure is fundamental as it imposes some constraints on the dynamics of passive tracers, which should be taken into account when carrying a numerical simulation.

2.4 Numerical settings

2.4.1 Charney-Hasegawa-Mima

Simulation of the Hasegawa-Mima equation are computed for different initial conditions and choices of the parameters. The choices made here corresponds largely to make them consistent with the literature, namely the conditions chosen in [3,15]. The simulations are performed within a square box of size $L = 20$ and periodic boundary conditions using a pseudo-spectral code. In order to compute the evolution of passive tracers accurately we settled for a somewhat low resolution mesh of 128^2 . Fourier transform are computed using a fast Fourier algorithm. For the time evolution, we chose a 4th-order Runge-Kunta integration scheme with typical time step $\Delta t = 0.05$.

In order to avoid numerical instability as well as a trivial asymptotic behavior Eq.(1) could not be kept as is and a dissipation term D as well as a forcing term F were added:

$$\partial_t + [;] = D + F; \quad (10)$$

One may also argue that the dissipation term may be relevant to describe some physical phenomena.

For the dissipation with considered a hyper-viscous term $D = (r)^4$, as for the forcing we used a term, which writes as follows in Fourier:

$$\hat{F}(k_x; k_y) = F_0 p \frac{1}{k^4} e^{i' (k_x; k_y)}; \quad (11)$$

where $i' (k_x; k_y)$ is a random phase uniformly distributed on the circle and is eventually time dependent and the values of k are centered around a value k_0 for a given k range.

The initial condition is given by the following choice for the $^0 =$ field:

$$^0 = A_0 \frac{x}{p \frac{1}{m^2 + n^2}} \sin \frac{2m}{L} x \frac{L}{2} \cos \frac{2n}{L} y +, \quad (12)$$

where i_{ij} is a random phase uniformly distributed on the circle.

2.4.2 Passive tracers

It is important to take special care of the way the dynamics of the tracers are computed to characterize the eventual anomalous properties of transport, which if present should find their origin in the existence of “memory effects”, namely long time correlations since the accessible range of speeds is finite. In this perspective, any source of randomness leading to memory loss due to the numerical scheme may then induce a spurious effective diffusive behavior. More over the Hamiltonian nature of the tracers dynamics imposes necessarily the choice of a symplectic integrator.

We thus chose the sixth-order implicit Gauss-Legendre symplectic scheme to compute the trajectories [23], as this integration scheme was successfully used in systems of point vortices [24,25,8,9]. However in order to avoid a possible source of noise, we needed to compute the speed of particles “exactly”, meaning that we performed an exact back-Fourier transform of the modes describing the evolution of the field. This constraint is numerically expensive, and explains our choice of a relatively low resolution of 128^2 for the evolution of the field. In this setting the evolution of passive tracers may be understood as describing the advection of particles in a flow field generated by 128^2 modes interacting through Eq.(1).

2.5 Field settings

When considering the evolution of equation (1) we are faced with a choice of parameters and initial conditions, our approach has been to consider three different cases, with quite different values of the parameters. As mentioned earlier on we chose as a starting base (initial condition, type of forcing, size of the system) similar conditions as those set in [3]. For the three cases considered, given

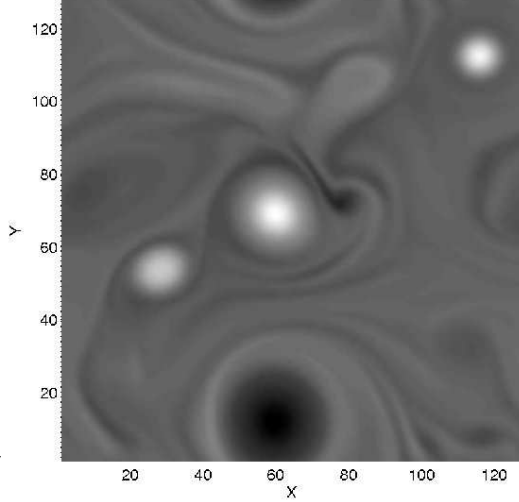


Fig. 1. Visualization of the field ψ for the choice of parameters $\epsilon = 1$, $g = 0.1$, $\eta = 7 \cdot 10^{-6}$, $L = 20$, $N = 128^2$ with no forcing. The field is “smooth” and appears as being isotropic. A few vortices are present. The gray coloring scheme scales from -4.5 (black) to 4.5 (white)

the initial condition we let the system evolve until it can be considered “stationary” for the time considered during simulation $t_{\text{final}} = 10^4$, stationarity considered being reached by monitoring the evolution of the energy and enstrophy of the system (see Table 1).

In order to visualize the field we chose to use levels of the function ψ . The three different cases considered are represented in figures 1, 2 and 3.

Table 1. Density of Energy and Enstrophy for the three considered cases

	Energy		Enstrophy	
Smooth Field	0.64	0.01	0.8	0.05
Forced Field	2.62	0.005	10.81	0.03
Anisotropic Field	0.28	0.005	0.18	0.01

2.5.1 Smooth Field

To obtain the “smooth” field depicted in Fig. 1, we carried out simulations with no forcing and low dissipation, the parameters for this run were $\epsilon = 1$, $g = 0.1$, $\eta = 7 \cdot 10^{-6}$. Due to this low dissipation the energy may be considered constant for the length of the simulation. We can notice that a few distinct vortices are present, during the evolution a merger between two vortices occur, one can also notice an average drift in the y -direction.

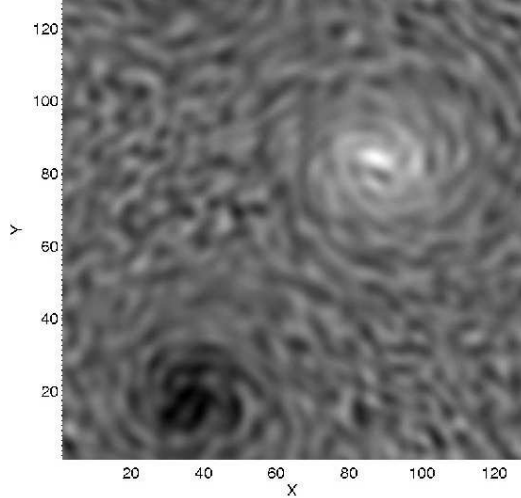


Fig. 2. Visualization of the field for the choice of parameters $\epsilon = 4$, $g = 0.1$, $\gamma = 5 \cdot 10^{-5}$, $F_0 = 4$, $k_0 = 6 \cdot 2$, $t = 2$. Two big perturbed vortices are present. The gray coloring scheme scales from -1.4 (black) to 1.4 (white)

2.5.2 Forced Field

To obtain the “forced” field depicted in Fig. 2, we carried out simulations with a strong forcing and dissipation, the parameters for this run were $\epsilon = 4$, $g = 0.1$, $\gamma = 5 \cdot 10^{-5}$, $F = 4$, $k_0 = 6 \cdot 2$, the phases for the random forcing are updated every $t = 2$ time units. The value of k_0 corresponds to physical scales of $x \approx \frac{2}{k_0} \approx 1$. With this choice of parameters the system consists of two perturbed vortices, an average drift in the y-direction is also noticeable.

2.5.3 Anisotropic Field

To obtain the “anisotropic” field depicted in Fig. 3, we carried out simulations with some forcing and a high value for g , the parameters for this run were $\epsilon = 0.125$, $g = 2$, $\gamma = 7.5 \cdot 10^{-6}$, $F = 1.5$, $k_0 = 12 \cdot 2$, $t = 2$. The value of k_0 corresponds to physical scales of $x \approx \frac{2}{k_0} \approx 0.5$. In this setting elongated structures as well as a strong drift in the y-direction is present.

3 Transport properties

3.1 Definitions

Unfortunately the deterministic description of the motion of a passive particle in a chaotic region is impossible. Local instabilities produce exponential divergence of trajectories, thus even an idealized numerical experiment is non-deterministic, as round-off errors are creeping slowly but steadily from the smallest to the observable scale. The long-time behavior of tracer trajectories is then necessarily studied by using a probabilistic approach. In the

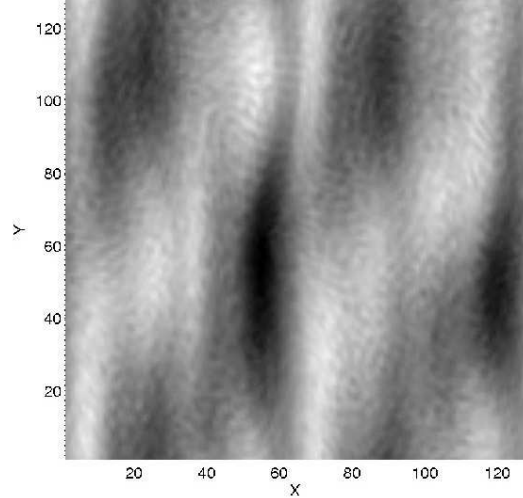


Fig. 3. Visualization of the field for the choice of parameters $\epsilon = 0.125$, $g = 2$, $\gamma = 7.5 \cdot 10^{-6}$, $F_0 = 1.5$, $k_0 = 12 \cdot 2$, $t = 2$. Elongated structures in the y-direction are present, marking a strong anisotropy. The gray coloring scheme scales from -1.6 (black) to 1.6 (white)

absence of long-term correlations, the kinetic description, which uses the Fokker-Plank-Kolmogorov equation, leads to Gaussian statistics. Yet if a phenomenon with associated long time correlations occurs, profound changes in the kinetics can be induced, when we are “lucky” these memory effects result in the modification of the diffusion coefficient in the FPK equation [26,27], but often their influence is more profound [28,29,30,7,8,9], and leads to non-Gaussian statistics and for instance a non-diffusive behavior of the particle displacement variance:

$$h(s) \approx h s^{\beta} i \quad t; \quad (13)$$

where h stands for ensemble averaging. For a superdiffusive case the transport exponent β exceeds the Gaussian value: $\beta > 1$. Within this probabilistic approach, the main observables in order to characterize transport properties will be moments of the distributions:

$$M_q(t) = h s^q(t) \approx h s(t) i^q i; \quad (14)$$

where q denotes the moment order. The physical restriction of a finite velocity and of a finite time of our simulations implies that all moments are finite and a power law behavior is expected

$$M_q \approx D_q t^{(q)}; \quad (15)$$

with, generally, $(q) \neq q=2$ as is expected from normal diffusion. The nonlinear dependence of (q) is a signature of the multifractality of the transport while its linear dependence reflects a fractal situation [30,31,32]. In the fractal situation all of the moments can be described by a single self-similar exponent β , i.e. (q) is linear

$$(q) = \beta q; \quad (16)$$

whereas the case when $\langle q \rangle$ is nonlinear, i.e. in (16) is not constant, i.e.

$$\langle q \rangle = q \langle q \rangle; \quad \langle q \rangle \notin \text{const} \quad (17)$$

transport is multifractal. This distinction is important since in the weak case the PDF must evolve in a self-similar way:

$$P(s; t) = t^{-f(\cdot)}; \quad t(s \text{ hsi}) \quad (18)$$

while a non-constant $\langle q \rangle$ in (17) precludes such self-similarity (see the discussions in [7,8] for details about the non self-similar behavior).

Before going on we insist on one last point; what we measure. We chose the arclength $s(t)$ of the path traveled by an individual tracer up to a time t ,

$$s_i(t) = \int_0^t v_i(t^0) dt^0; \quad (19)$$

where $v_i(t^0)$ is the absolute speed of the particle i at time t^0 . We recall that in order to consider mixing properties from the dynamical principles it is important to consider the trajectories within the phase space. However, for the considered case the phase space is “identical” to the physical space where particles evolve (see Eq.9). One advantage of this quantity is that it is independent of the coordinate system and as such we can expect to infer intrinsic properties of the dynamics.

Moreover, the expression (19) we directly see that the value of $s_i(t)$ is directly correlated to the history up to time t of the speed v_i and since the speed support is bounded the observations described further on of anomalous transport behavior are directly linked to strong memory effects.

3.2 Particles Transport

As mentioned in order to study the transport properties of passive tracers in Charney-Hasegawa-Mima flows, we considered three different cases with different choices of parameters and forcing. In these field we followed the evolution of 512 passive particles given by Eq.(8), and measured the arclength $s_i(t)$ travelled by each tracer i , up to a time $t = 10^4$. In order to keep a constant accuracy the increments $s_i(t)$ were recorded for successive diagnostic times. This last feature has also the advantage of allowing better statistics when computing moments. Indeed since we have chosen stationary regimes for the field, we can assume that transport properties are independent from the initial condition of the field and thus use time-invariance to increase statistics.

In all three considered cases the transport is found to be anomalous and superdiffusive, with a characteristic second order exponent all of the same order $\langle 2 \rangle = 1.8$. An illustration of such behavior of the second moment versus time is illustrated in Fig.4 where the data obtained from the anisotropic case is used. The time behavior of the moments and characteristic exponents for all considered cases

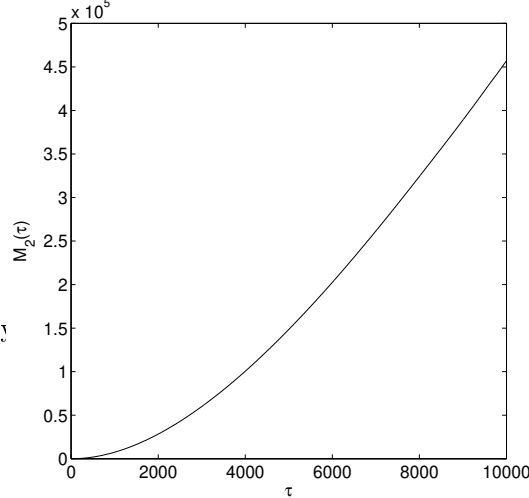


Fig. 4. Evolution of the second moment of the distribution of arclength $M_2(\cdot) = \langle s^2(\cdot) \rangle$ of tracers evolving in the anisotropic field. The non-Gaussian behavior $M_2(\cdot) \propto t^{1.85}$ is illustrated, transport is anomalous.

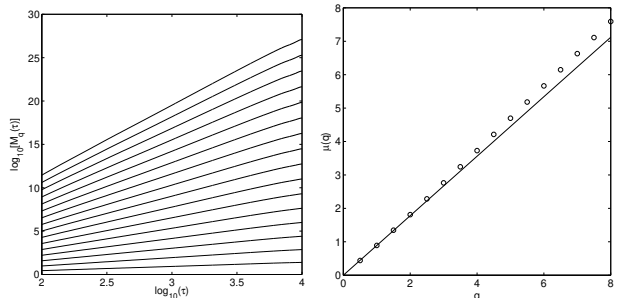


Fig. 5. Left: Moments of distribution of the arclength $M_q(\cdot) = \langle s^q(\cdot) \rangle$ versus time of tracers evolving in the smooth field for $q = 1=2; 1; 3=2; \dots; 8$. The behavior $\langle M_q \rangle \propto t^{(q)}$ is confirmed. Right: Characteristic exponent versus moment order, q vs $\langle q \rangle$, with $\langle 2 \rangle = 1.81$. Transport is super-diffusive and multifractal.

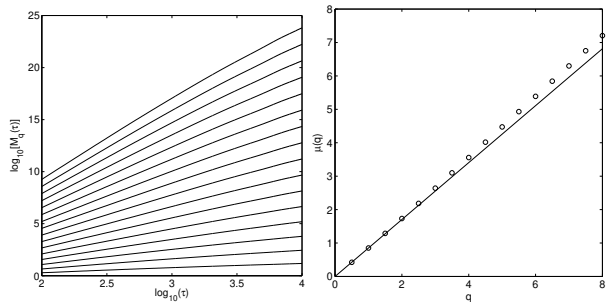


Fig. 6. Left: Moments of distribution of the arclength $M_q(\cdot) = \langle s^q(\cdot) \rangle$ versus time of tracers evolving in the forced field for $q = 1=2; 1; 3=2; \dots; 8$. The behavior $\langle M_q \rangle \propto t^{(q)}$ is confirmed. Right: Characteristic exponent versus moment order, q vs $\langle q \rangle$, with $\langle 2 \rangle = 1.73$. Transport is super-diffusive and multifractal.

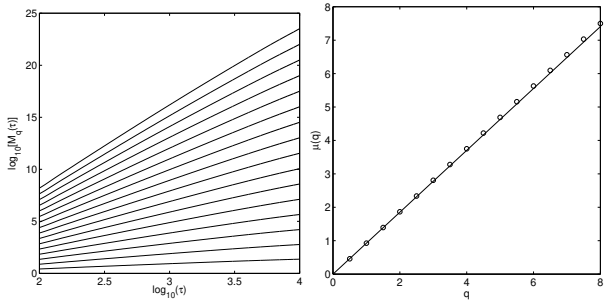


Fig. 7. Left: Moments of distribution of the arclength $M_q(t) = \int ds(t) \delta^2(s, t)$ versus time of tracers evolving in the anisotropic field for $q = 1=2; 1; 3=2; \dots, 8$. The behavior is confirmed. Right: Characteristic exponent versus moment order, q vs $\log_{10}(q)$, with $\log_{10}(2) = 1.39$. Transport is super-diffusive and single fractal.

Table 2. Characteristic second moment exponent for the three different cases studied. Exponents obtained in flows governed by point vortices in Ref. [9] are given for comparison.

Point vortices	4 vortices	$\log_{10}(2)$	1.82
	16 vortices	$\log_{10}(2)$	1.77
Charney-Hasegawa-Mima	Smooth Field	$\log_{10}(2)$	1.81
	Forced Field	$\log_{10}(2)$	1.73
	Anisotropic Field	$\log_{10}(2)$	1.85

are plotted in figures 5, 6 and 7 and a summary is provided in table 2, where we included for comparison the results obtained in Ref. [9] for a flow governed by point vortices. The similarity observed for the exponents in these quite different settings of the parameters and regimes of the Charney-Hasegawa-Mima equation as well as the one observed in point vortices, raises the possibility of some kind of universal behavior for the transport of passive tracers in these two-dimensional flows.

However conversely to the point vortices case, one can notice from Figs. 5, 6 and 7 that the behavior of characteristic exponent versus moment order corresponds to multifractal transport in the first two cases but the nonlinear dependence is quite weak, and to simple fractal transport in the anisotropic system. This last feature implies an almost self-similar behavior of the distribution function, and that transport properties in this system should be correctly described by a fractional Fokker-Plank-Kolmogorov equation of the type [6]:

$$\frac{\partial P(s, t)}{\partial t} = D \frac{\partial P(s, t)}{\partial s_j} : \quad (20)$$

4 Jets

4.1 Definitions

Tracking the origin of anomalous transport can be fairly well understood when one is able to draw a phase portrait using a Poincaré map and for instance measuring Poincaré return time to a given region of the phase space. The conclusion of this type of analysis will almost certainly lead to

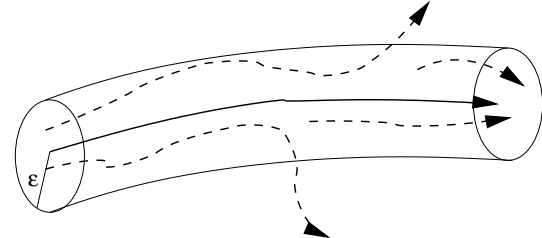


Fig. 8. Tracking of coarse-grained regular jet.

the fact that the phenomenon of stickiness on the boundaries of the islands generates strong “memory effects” as a result of which transport becomes anomalous. However, when dealing with a more complex systems, for which the drawing of a phase portrait is not achievable, one has to rely on other techniques.

In a two dimensional phase-space, the phenomenon of stickiness corresponds often to passive particles remaining for large times in the neighborhood of an island of regular motion. A consequence of this behavior is that sticky zones are regions where particles are trapped and therefore are regions where particles remain in each others neighborhood for large times. It becomes therefore natural when dealing with more complex systems for which no phase portrait can easily be drawn to look for places where passive particles remain in each other’s vicinity for large times. One possibility to achieve this feature of the dynamics is to look for its signature by measuring finite time Lyapunov exponents (FTLE) and by isolating within the space of initial conditions regions of vanishing FTLE’s (see for instance [33]). This type of approach has however its shortcoming, namely sticky regions are not necessarily smooth from the microscopic point of view, meaning they can be region of strong chaos that are somehow restricted within an arbitrary small scale, which may be problematic when dealing with FTLE’s. The other possibility is to look directly for chaotic jets [9]. These chaotic jets can be understood as moving clusters of particles within a specific domain for which the motion appears as almost regular from a coarse grained perspective. From another point of view, looking for chaotic jets can be understood as a particular case of measurements of space-time complexity[12].

In order to look for jets we proceed as described in the illustration presented in Fig. 8 which provides an easy and intuitive description of the mechanism used to detect jets. To resume, we consider a reference trajectory $r(t)$ within the phase space. We then associate to this trajectory a corresponding “coarse grained” equivalent, i.e the reunion of the balls $[B(r(t); \epsilon)]$ of radius ϵ whose center is the position $r(t)$. Given an ϵ -coarse grained trajectory, we analyze the behavior of real trajectories starting from within the ball at a given time and measure the time τ and length s , corresponding to actually how long the trajectory remains and how much it travels before its first escape from the coarse grained trajectory. We then analyze the resulting distributions. This approach has already been used with success when studying numerically the advection of pas-

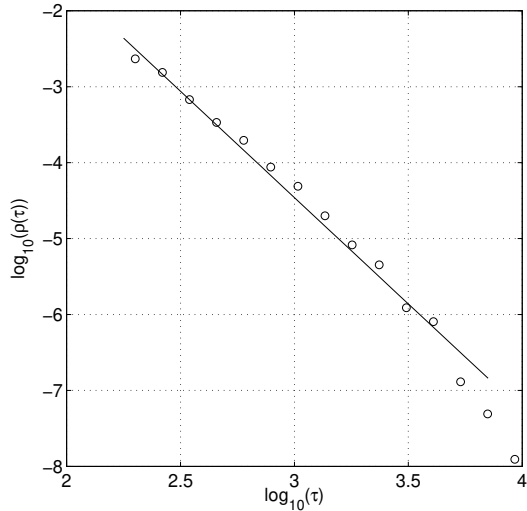


Fig. 9. Tail of the distribution of trapping times for the smooth field (Fig. 1). A power-law decay is observed with typical exponent () with 2.8 ± 0.1 . Case1

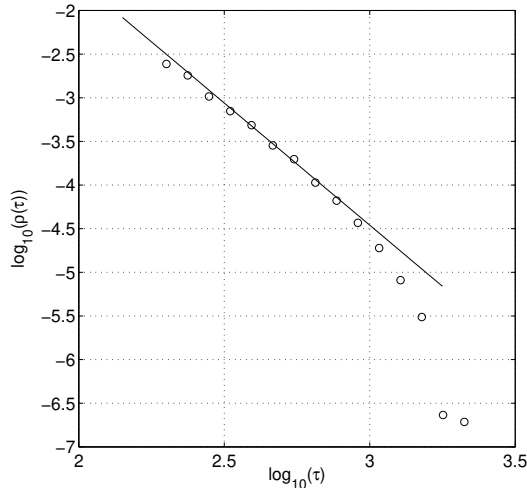


Fig. 10. Tail of the distribution of trapping times for the forced field (Fig. 2). A power-law decay is observed with typical exponent () with 2.8 ± 0.1 .

sive tracers in flows governed by point vortices [9]. The main difficulty in using this diagnostic follows from the fact that data acquisition is not sampled linearly in time nor space, a point which lead in the present case to some difficulties.

4.2 Statistical results

In the setting of the evolution of passive tracers within the three considered Charney-Hasegawa-Mima flows, we settled for the following values $\tau = 10^1$ and $\tau = 10^3$, these values are to be compared with the $\tau = 10^2$ and $\tau = 10^6$ considered for point vortex systems in [9]. This reduction of accessible scales stems from the fact that for the length of our simulations ($\tau = 10^4$) and trying to use the point

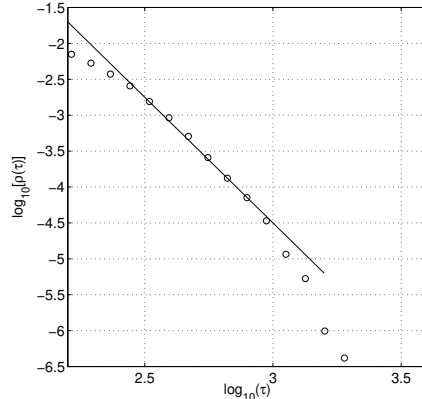


Fig. 11. Tail of the distribution of trapping times for the anisotropic field (Fig. 3). A power-law decay is observed with typical exponent () with 3.5 ± 0.5 .

vortex values, only a few trajectories are escaping from the jets, leaving us with not enough data to gather realistic statistics. With the modified choice of parameters we were able to gather about 15000 events for each of the three cases by following 256 reference trajectories for which the behavior of two nearby tracers was checked for a time $\tau = 10^4$. We were then able to obtain the trapping time distributions () described in Figs. 9, 10 and 11. The characteristic exponent () for trapping times observed in two out of the three systems is typically 2.8 . For these cases we can therefore a good agreement with the

$$(2) \quad 1; \quad (21)$$

relation which links the transport exponent α to the characteristic trapping time exponent (see [8,9] for a derivation of this law). In fact the law (21) also applies in the anisotropic field for small trapping times, hence we speculate it would be recovered if we were able to carry simulations for larger times. Indeed for this configuration of the field the energy and enstrophy are quite low, implying weak nonlinear effects, it may thus take more time to fill the tail of the trapping time distribution. Another peculiarity of the anisotropic case is the simple fractal signature of transport seen in Fig. 7. In fact as pointed out in [34,35], in the anisotropic case, the conservation of the generalized vorticity by the evolution of the Hasegawa-Mima equation implies necessarily that for strong values of g the motion along the x direction is bounded. Hence in this situation the motion of passive tracers is quasi one-dimensional, which could explain the single fractal structure of transport as well as the difficulty to track long lived jets in this setting.

The rarefaction of events with smaller values of τ indicates that the trajectories of tracers are relatively regular when one considers small scales, which implies the possibility of vanishing Lyapunov exponents. Hence, following the definitions given in [9]:

$$\alpha_L = \frac{1}{\tau} \ln \frac{1}{\rho(\tau)}; \quad (22)$$

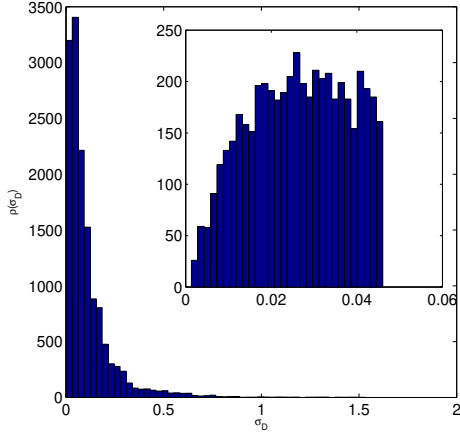


Fig. 12. Unnormalized Distribution of Lyapunov exponents σ_D , see Eq. (23). An accumulation towards zero is observed. The zoom near small regions reveals an actual decrease for $\sigma_D < 0.02$, such behavior is expected as data is bounded by finite speed and finite time.

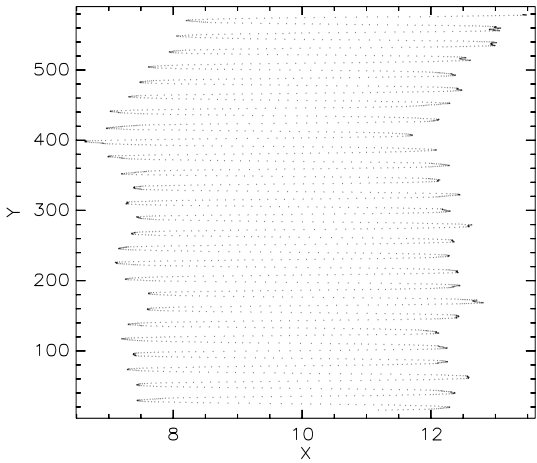


Fig. 13. Localization of a long lived jet in the “Forced Field” (cf Fig. 2). The jet is bouncing back and forth between the two perturbed vortices

$$\sigma_D = \frac{1}{s} \ln - ; \quad (23)$$

we compute the distribution of Lyapunov exponents σ_D obtained from the smooth case data in Fig. 12, where one can directly see an accumulation towards zero of the distribution. The zoom in Fig. 12 shows an actual decrease for $\sigma_D < 0.02$. This behavior is expected as we only have finite speeds in the system and simulations simulations are carried for a finite time, for instance $\sigma_D < 0.02$ corresponds to an average trapping time $t_a = 1100$.

4.3 Localization and structure of jets

Due to the shape of the finite size Lyapunov exponent distributions observed, it is also possible to track and localize jets which are responsible for the anomalous behavior. Indeed, these exponents are monotonously decreasing hence

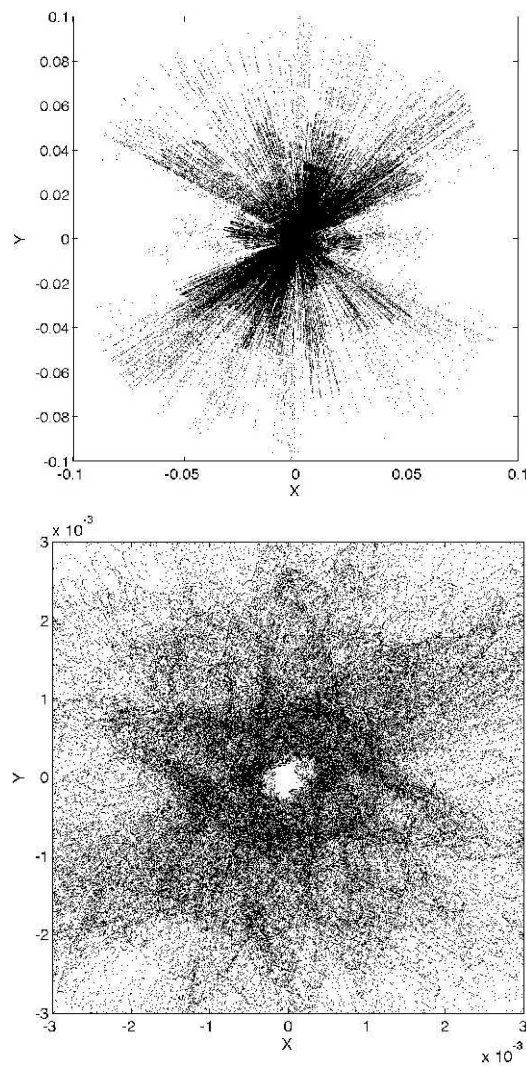


Fig. 14. Relative position of test particles for the long lived jet depicted in Fig. 13 (top). Zoom (bottom), test particles reach distances $< 10^{-4}$ to the reference trajectory.

we can define threshold beyond which the jet can be considered “regular” and track the reference trajectory afterwards in order to localize regions responsible for anomalous behavior. In Fig. 13 we show the localization of a jet for which the trapping time of nearby tracers are found to be ~ 1000 , in the case of the forced field (cf Fig. 2). The jet is bouncing back and forth between the two perturbed vortices.

Once a jet is located one can infer the behavior of the test tracers with respect to the reference trajectory. In order to get Fig. 14, 256 test particles were initialized on a circle around a reference particle whose trajectory was trapped in a long lived jet and the relative positions of the test particles were plotted during the life of the jet. The “star” like shape of the figure in is the consequence of multiple stretching and squeezing of the circle of particles, which one can observe while looking dynamically at the evolution of the circle. This behavior reflects the

fact that despite the trajectories within the jet are likely chaotic, their chaotic behavior is trapped within a given small scale for a long time, giving rise to a regular non-diffusive trajectory from a coarse grained perspective.

5 Conclusion

In this paper we have investigated the dynamical and statistical properties of passive particles advection in different configurations of Charney-Hasegawa-Mima flows. The goal of the work was to consider transport properties of these systems while putting in perspective the results obtained for point vortex flows. In this sense it was a step further in providing qualitative insights on general transport properties of two-dimensional flows. The transport properties of all the considered cases are found to be anomalous with characteristic exponent 1.75 ± 1.8 , these values are also quantitatively comparable to the results obtained for point vortex flows.

In order to analyze the origin of the anomalous transport properties, passive tracer motion is analyzed by measuring the mutual relative evolution of two nearby tracers, i.e by looking for chaotic jets [9]. The jets can be understood as moving clusters of particles within a specific domain where the motion is almost regular from a coarse grained perspective inducing memory effects and long time-correlations. The distribution of trapping times in the jets shows a power-law tail whose characteristic exponent is in very good agreement with the law $\tau = \tau_0 + t$ linking the transport exponent α to the trapping time exponent β . This agreement is a good signature that the origin of anomalous transport in these system is intimately related to the existence of jet in the sense described previously. The localization of jets in the system can be done, and it is shown that jets are not necessarily located around a coherent structure as was the case for point vortex flows, but that they can manifest themselves by a trajectory bouncing back and forth between 2 structures. Moreover when analyzing the “structure” of the jet, it is shown that the trajectory of individual tracers are likely chaotic within the jet, but that this chaotic behavior is for long times restricted within a given small scale, giving rise to the regular non-diffusive structure.

Part of the work presented in this paper was carried out while X.L was visiting the Department of Fundamental Energy Science, Graduate School of Energy Science, Kyoto University. X.L thanks S. Hamaguchi and A. Bierwage for useful discussions as well as the Department for its financial support. G.M.Z. was supported by the U.S. Navy Grant N00014-96-1-0055 and the U.S. Department of Energy Grant No. DE-FG02-92ER54184.

References

1. M. F. Schlesinger, G. M. Zaslavsky, and J. Klafter. *Nature*, 363:31, 1993.
2. B. A. Carreras, V. E. Lynch, L. Garcia, M. Edelman, and G. M. Zaslavsky. Topological instability along filamented invariant surfaces. *Chaos*, 13(4):1175, 2003.
3. S. V. Annibaldi, G. Manfredi, R. O. Dendy, and L. O'C. Drury. Evidence for strange kinetics in hasegawa-mima turbulent transport. *Plasma Phys. Control. Fusion*, 42:L13–L22, 2000.
4. D. del Castillo-Negrete, B. A. Carreras, and V. E. Lynch. Fractional diffusion in plasma turbulence. *Phys. Plasmas*, 11(8):3584, august 2004.
5. V. Grandgirard, O. Agullo, S. Benkadda, B. Biehler, X. Garbet, P. Ghendrih, and Y. Sarazin. Impurity transport in flux driven models of edge turbulence. *Proceedings of the Varenna conference, "Theory of Fusion Plasmas"*, Editors J.W. Connor, O. Sauter and E. Sinden, pages 427 – 432, 2000.
6. G. M. Zaslavsky. Chaos, fractional kinetics, and anomalous transport. *Phys. Rep.*, 371:641, 2002.
7. L. Kuznetsov and G. M. Zaslavsky. Passive particle transport in three-vortex flow. *Phys. Rev. E*, 61:3777, 2000.
8. X. Leoncini, L. Kuznetsov, and G. M. Zaslavsky. Chaotic advection near 3-vortex collapse. *Phys. Rev. E*, 63(036224), 2001.
9. X. Leoncini and G. M. Zaslavsky. Jets, stickiness and anomalous transport. *Phys. Rev. E*, 65(046216), 2002.
10. V. V. Afaniasiev, R. Z. Sagdeev, and G. M. Zaslavsky. Chaotic jets with multifractal space-time random walk. *Chaos*, 1:143, 1991.
11. Xavier Leoncini and George M. Zaslavsky. Chaotic jets. *Communications in Nonlinear Science and Numerical Simulation*, 8:265–271, 2003.
12. V. Afraimovich and G. M. Zaslavsky. Space-time complexity in hamiltonian dynamics. *CHAOS*, 13(2):519–532, June 2003.
13. A. Hasegawa. *Adv. Phys.*, 34, 1981.
14. J. Pedlosky. *Geophysical Fluid Dynamics*. Springer-Verlag, New-York, 1987.
15. S. V. Annibaldi, G. Manfredi, and R. O. Dendy. Non-gaussian transport in strong plasma turbulence. *Phys. Plasmas*, 9(3):791, March 2002.
16. V. Naulin, A. H. Nielsen, and J. Juul Rasmussen. Dispersion of ideal particles in a two dimensional model of electrostatic turbulence. *Phys. Plasmas*, 6(12):4575, 1999.
17. R. Dickman. Fractal rain distributions and chaotic advection. *Brazilian Journal of Physics*, 34:337, 2004.
18. F. Dupont, R. I. McLachlan, and V. Zeitlin. On possible mechanism of anomalous diffusion by rossby waves. *Phys. Fluids*, 10(12):3185, december 1998.
19. J. Sukhatme. Lagragian velocity correlations and absolute dispersion in the midlatitude troposphere. *J. Atmos. Sci.*, *arXiv:physics/0410130*, submitted, 2004.
20. P. Beyer and S. Benkadda. Advection of passive particles in the kolmogorov flow. *Chaos*, 11(4):774, December 2001.
21. O. Agullo and A. Verga. Relaxations towards localized vorticity states in drift plasmas and geostrophic flows. *Phys. Rev. E*, 69:056318, 2004.
22. C.F. Fontán and A. Verga. Dynamics of coherent structures and turbulence of plasma drift waves. *Phys. Rev. E*, 52:6717, 1995.
23. R.I. McLachlan and P. Atela. The accuracy of symplectic integrators. *Nonlinearity*, 5:541, 1992.
24. L. Kuznetsov and G. M. Zaslavsky. Regular and chaotic advection in the flow field of a three-vortex system. *Phys. Rev E*, 58:7330, 1998.

25. A. Laforgia, X. Leoncini, L. Kuznetsov, and G. M. Zaslavsky. Passive tracer dynamics in 4 point-vortex-flow. *Eur. Phys. J. B.*, 20:427, 2001.
26. B. V. Chirikov. Universal instability of many-dimensional oscillator systems. *Phys. Rep.* 52, 52:263, 1979.
27. A.B. Rechester and R. White. Calculation of turbulent-diffusion for the chirikov-taylor model. *Phys. Rev. Lett.*, 44:1586, 1980.
28. G.M. Zaslavsky, D. Stevens, and H. Weitzner. Self-similar transport in incomplete chaos. *Phys. Rev E*, 48:1683, 1993.
29. D. del Castillo-Negrete. Asymmetric transport and non-gaussian statistics of passive scalars in vortices in shear. *Phys. Fluids*, 10:576, 1998.
30. P. Castiglione, A. Mazzino, P. Mutatore-Ginanneschi, and A. Vulpiani. On strong anomalous diffusion. *Physica D*, 134:75, 1999.
31. K. H. Andersen, P. Castiglione, A. Massino, and A. Vulpiani. Simple stochastic models showing strong anomalous diffusion. *Eur. Phys. J. B*, 18:447, 2000.
32. R. Ferrari, A. J. Manfroi, and W. R. Young. Strong and weakly self-similar diffusion. *Physica D*, 154:111, 2001.
33. S. Boatto and R. T. Pierrehumbert. Dynamics of a passive tracer in a velocity field of four identical point vortices. *J. Fluid Mech.*, 394:137, 1999.
34. R. Basu, T. Jessen, V. Naulin, and J. J. Rasmussen. Turbulent flux and the diffusion of passive tracers in electrostatic turbulence. *Phys. Plasmas*, 10(7):2696, 2003.
35. R. Basu, V. Naulin, and J. J. Rasmussen. Particle diffusion in anisotropic turbulence. *Communications in Nonlinear Science and Numerical Simulation*, 8:477–492, 2003.